2013 IEEE/RSJ International Conference on
Intelligent Robots and Systems (IROS)
November 3-7, 2013. Tokyo, Japan

Nearly fuel-optimal trajectories for vehicle swarms in open domains with strong background flows

Doug Lipinski[1,3] and Kamran Mohseni[1,2,3]

Abstract— **Using a multi-vehicle control scheme based on smoothed particle hydrodynamics, a simulated swarm of unmanned underwater vehicles is guided along a pre-computed optimal trajectory between two points in an open domain under the influence of a strong background flow. The pre-computed trajectory is optimal in terms of fuel usage for a single vehicle. If the gradient of the velocity field is small compared to the total swarm radius, guiding a swarm of vehicles along this trajectory gives nearly optimal trajectories for all vehicles in the swarm without requiring additional costly optimization computations. We provide a bound on the maximum energy cost for vehicles in the swarm and also provide a more realistic estimate of the maximum energy cost. We also determine that the energy cost scales as $N^{3/2}$ for swarms with large numbers of vehicles, N. The algorithm and fuel cost bounds are verified in simulations of unmanned underwater vehicles moving across a double gyre system on the scale of a small ocean basin.**

I. Introduction

The problem of guiding a vehicle or vehicles through open domains with large background velocity fields (relative to vehicle speed) is common in the field of oceanic sensing and monitoring. For example, underwater gliders used in ocean research may operate autonomously for months at a time, traveling up to thousands of kilometers with speeds of only about 25 cm/s [1]. The long term, relatively low cost measurement capabilities of such gliders is largely made possible by their very low speed, which requires very little power to operate, only about 0.5 W [1]. However, these low power capabilities come at the cost of vehicle speed. In many cases, ocean currents reach speeds of around 1 m/s, making certain regions inaccessible to the vehicles unless careful path planning techniques are used.

While there is a large body of existing research on optimal path planning in static and dynamic environments, the vast majority of this work is focused on ground robots where a path must be planned to avoid physical obstacles [2], [3], [4]. On the contrary, there are relatively few results on optimal path planning through dynamic, strong background flows. Past work in this area has noted the apparent connection between optimal trajectories and coherent structures in oceanic flows [5], [6] and a recent algorithm has been developed to determine minimum time trajectories for a single underwater vehicle in an open domain [7].

In this investigation, we focus on generating nearly fuel-optimal trajectories for large swarms of vehicles in open domains with strong background flows. As discussed above, underwater vehicles in the ocean may greatly benefit from fuel-optimal trajectory planning. Additionally, as underwater vehicles become cheaper, it may be more common to release large groups of vehicles to travel as a swarm and maximize information gathering capabilities.

Given a good prediction of the background velocity in the domain of interest, it is reasonable to formulate an optimization problem for a single vehicle traveling between two points subject to certain motion constraints. Typically, one may wish to minimize the fuel usage, travel time, or some combination of the two. For a single vehicle, this optimization problem may be solved in many ways, however, as additional vehicles are added to the system, the necessity of ensuring collision avoidance and reasonable swarm behavior quickly makes the problem intractable, especially if swarms of dozens or even hundreds of vehicles are used.

To address the growing complexity of the optimization problem, we achieve nearly optimal trajectories for a vehicle swarm by guiding an entire swarm of vehicles along a trajectory that is optimal for a single vehicle. The center of the swarm remains very close to the optimal trajectory, but vehicle's at the margins of the swarm are farther away from this optimal path. As long as the velocity gradients in the background flow are small compared to the total swarm size, all vehicles in the swarm achieve a nearly optimal trajectory.

To address the vehicle guidance issues associated with large swarms of vehicles, we use a smoothed particle hydrodynamics (SPH) based control scheme. This control scheme treats each vehicle in the swarm as an individual fluid particle, providing obstacle and collision avoidance while allowing for simple, distributed computing.

To analyze the effectiveness of this control scheme, we provide a bound on the swarm fuel cost based on the swarm moving as a rigid body along the optimal trajectory based on the swarm size and the gradients in the background velocity field. We also present the results of simulations based of underwater vehicles moving across a double gyre flow on the scale of a small ocean basin. Realistic vehicle constraints are enforced and it is verified that the swarm obeys the upper bound on fuel cost for groups ranging in size from one to 500 vehicles. Additionally, it is observed that the average fuel cost per vehicle grows only as $N^{3/2}$ for large numbers of vehicles in the swarm.

The primary contribution of this paper is the introduction and validation of a new method for nearly-optimal swarm guidance in background flows. We provide a bound on the

[1]Dept. of Aerospace and Mechanical Engr, University of Florida
[2]Dept. of Electrical and Computer Engr, University of Florida
[3]Institute for Networked Autonomous Systems, University of Florida

978-1-4673-6357-0/13/$31.00 ©2013 IEEE

fuel consumption which proves that the trajectories are nearly optimal as long as the velocity gradients in the background flow are small on the scale of the swarm size. Additionally, we provide a more useful (i.e. more accurate) estimate for the actual energy costs as well as a parametric model for the cost as a function of number of vehicles in the swarm. We find that the parametric model provides very good estimates for fuel usage when extrapolating to large swarms (up to 500 vehicles) based on simulations of moderately sized swarms ($N \leq 100$).

II. Smoothed Particle Hydrodynamics

While there are many possible choices available for cooperative control algorithms, we have chosen to use a control scheme based on smoothed particle hydrodynamics (SPH). SPH is simple to implement, computationally efficient, and gives fluid-like swarm movement. SPH is a Lagrangian formulation of the Navier-Stokes equations of fluid motion. In the context of cooperative control, each vehicle is treated as a fluid particle. Pressure forces provide collision avoidance and viscous forces provide a consensus term between vehicles. Additionally, it is possible to create virtual reduced density particles to provide guidance to groups of vehicles. Just as fluid flows toward regions of low pressure, these virtual particles act as goals or attractors for other SPH particles. For compactness, we review only the necessary components of the SPH formulation here. The reader is referred to the article by Monaghan [8], the book by Liu and Liu [9], or the references therein for further details.

In the SPH formulation, the acceleration of a vehicle is determined by its interactions with nearby vehicles. The range of interactions is limited by the use of a smoothing kernel through which all fluid properties are applied and the resulting accelerations are computed. There are many smoothing kernels available, given various properties that may be desirable for different purposes. In general, the smoothing kernel is gaussian-like and we also chose a compactly supported kernel to limit the range of vehicle interactions. We choose the kernel function

$$W(\mathbf{r},h) = \frac{C}{h^d}\begin{cases} 1-\frac{3}{2}s^2+\frac{3}{4}s^3 & \text{if} \quad 0 \leq s \leq 1 \\ \frac{1}{4}(2-s)^3 & \text{if} \quad 1 < s \leq 2 \\ 0 & \text{if} \quad s > 2 \end{cases} \tag{1}$$

where $\mathbf{r}$ is the position vector, h is the smoothing length, d is the dimension of the space (2 or 3), C is a normalization constant such that $\int W d\mathbf{x} = 1$ and $s = ||\mathbf{r}||_2/h$.

Apply this SPH assumptions to the Navier-Stokes equations of fluid motion gives rise to

$$\rho_i = \sum_j W(\mathbf{r}_{ij},h)m_j, \tag{2}$$

$$\begin{aligned}\frac{d\mathbf{v}_i}{dt} = &-\sum_j m_j\left(\frac{P_i}{\rho_i^2}+\frac{P_j}{\rho_j^2}+\Pi_{ij}\right)\nabla_i W(\mathbf{r}_{ij},h) \\ &+\sum_j m_j \frac{2\mu}{\rho_i\rho_j}\frac{\mathbf{v}_{ij}}{r_{ij}}\frac{dW}{dr_{ij}},\end{aligned} \tag{3}$$

where ρ is density, m is mass, $\mathbf{v}$ is velocity, P is pressure, ∇_i is the gradient with respect to particle i, $\mathbf{r}_{ij} = \mathbf{r}_j - \mathbf{r}_i$, μ is viscosity, subscripts denote particle identity, $\mathbf{v}_{ij} = \mathbf{v}_j - \mathbf{v}_i$, and $r_{ij} = ||\mathbf{r}_{ij}||_2$. The mass is chosen so that particles have neutral density in isolation, i.e.

$$m_i = \frac{\rho_0}{W(0,h)}. \tag{4}$$

This mass ensures that vehicles always experience a repelling force when $r_{ij} < 2h$. The pressures must be computed using an equation of state such as

$$P_i = K\rho_i\left(\frac{\rho_i}{\rho_0}-1\right). \tag{5}$$

The coefficients μ, K, and ρ_0 must be determined by other means. In fluid simulations, these coefficients are related to the physical properties of the fluid, i.e. the viscosity, the bulk modulus, and a reference density. However, we must choose these parameters in a different way for the purpose of cooperative control.

In the context of cooperative control, the accelerations computed through the SPH equations are the desired accelerations of the vehicles in the swarm. Obviously this leads to some constraints on the realistically achievable accelerations and velocities. In the past, there has not been a clear way of systematically choosing the values of μ, K, and ρ_0 to give accelerations that are of the desired magnitude for the vehicles. A common issues was the appearance of a bang-bang controller where the acceleration magnitudes are either zero or the maximum possible value. This results from K and mu being too large. If the mass is chosen as in equation (4), it is possible to factor and cancel ρ_0 from every term in the equations so the choice of ρ_0 has no affect on the solution. For simplicity, we simply set $\rho_0 = 1$ in all future computations. We must then scale K and μ to achieve the desired behavior.

We begin by considering the desired behavior qualitatively in terms of a Reynolds number. The Reynolds number is defined as the ratio of inertial forces to viscous forces and in fluid flows is given by

$$Re = \frac{\rho_0 L v_0}{\mu} \tag{6}$$

for a reference length scale L and speed v_0. In the cooperative control scheme, this ratio still applies, but now the inertial forces are generated by the repulsive pressure force terms and the viscous forces create a velocity consensus type term. Typically, collision avoidance is significantly more important than velocity consensus so we have found that a Reynolds number of around $Re = 10$ is usually appropriate.

We can directly compare the pressure forces and the viscous forces between two particles separated by a distance h with a velocity difference of v_{max}. This gives a pressure force (per unit mass) of

$$F_p = \left|2K\frac{W(h,h)}{W(0,h)(W(0,h)+W(h,h))}\frac{dW(h,h)}{dr_{ij}}\right| \tag{7}$$

and a viscous force (per unit mass) of

$$F_\mu = \left| 2\mu \frac{W(0,h) v_{\max}}{(W(0,h) + W(h,h))^2} \frac{dW(h,h)}{dr_{ij}} \right|. \quad (8)$$

The ratio of these two forces gives

$$Re = \frac{F_p}{F_\mu} \quad (9)$$

Additionally, the vehicles typically have a maximum acceleration that is related to the turning radius. For vehicles with a turning radius of $R_{\min}$ at a speed of $v_{\max}$, the maximum acceleration is given by

$$a_{\max} = \frac{v_{\max}^2}{R_{\min}}. \quad (10)$$

The total acceleration given by the SPH equations should be approximately the same as $a_{\max}$, giving

$$a_{\max} = F_p + F_\mu. \quad (11)$$

Finally, we solve equations (7) and (8) for K and μ for the vehicle particles.

Swarm guidance is handled through the use of virtual particles with reduced density. These virtual particles may be added, subtracted, or moved around the domain as needed. They also typically have a much large smoothing width h than the vehicle particles so that their attraction force acts over a large distance. As long as the virtual particle density is less than the reference density the pressure will be negative at the attracting particle, causing attracting forces. For simplicity, we use a fixed zero mass limit to determine the forces due to the virtual reduced density particles. Additionally, these particles to not exert any viscous forces, doing so would act in opposition to the motion of vehicles toward the virtual particle. In the limit of zero mass for a reduced density virtual particle, we find that the an isolated vehicle particle experiences acceleration of

$$F_{\text{r.d.}} = \frac{K_{\text{r.d.}}}{W(0, h_{\text{r.d.}})} \nabla W(\mathbf{r}, h_{\text{r.d.}}) \quad (12)$$

where subscript r.d. denotes properties specific to the reduced density particle and $\mathbf{r}$ is the vector from the vehicle particle to the attractor particle. Again, based on the on the maximum vehicle acceleration we can find $K_{\text{r.d.}}$ by solving

$$a_{\max} = \alpha F_{\text{r.d.}} \quad (13)$$

Here, we choose a constant $0 < \alpha \leq 1$ so that forces from the attractor particle are typically less than the forces between vehicles that provide collision avoidance which is a higher priority. Values of $\alpha = 0.1 - 0.5$ typically seem to work well.

By choosing the SPH parameters using the methods outlined in this section, we ensure the qualitative behavior desired by the choice of Reynolds number while also ensuring that the desired accelerations are of the same order as the vehicle capabilities. This eliminates the bang-bang control results that we have experienced with other choices of SPH parameters. Finally, we compute the final vehicle acceleration, $\ddot{\mathbf{x}}$, via

$$\ddot{\mathbf{x}} = \text{constrain}\left(c_1 \frac{d\mathbf{v}}{dt} - c_2 \dot{\mathbf{x}} \right). \quad (14)$$

The addition of a drag force, $-c_2\dot{\mathbf{x}}$, increases the stability of the controller and helps to eliminate oscillations while the inclusion of the coefficients c_1 and c_2 allows for easy adjustments of the effects of the SPH forces and the drag force. Finally, a constraint function is applied to ensure that the final acceleration values and the resulting velocities are within the limits of the vehicle capabilities.

III. Optimal Trajectories

The end goal of this technique is guide vehicles along an nearly optimal trajectory through a complex, dynamic background velocity field. In order to do so, we must first define the optimization problem. Here, we consider only fuel-optimal trajectories by minimizing the fuel or energy cost along the trajectory. We assume that the drag on the vehicles is the primary energy cost and that this force is proportional to the vehicle speed squared. Let the vehicle velocity be given by $\dot{\mathbf{x}}$ and the background flow velocity be given by $\mathbf{U}$, then the normalized power usage (normalized by the maximum vehicle power) is given by

$$P(t) = \frac{||\dot{\mathbf{x}} - \mathbf{U}||_2^3}{v_{\max}^3} \quad (15)$$

and the total normalized energy (or equivalently, fuel) cost is given by

$$E = \int_{t_0}^{t_f} P(t) dt. \quad (16)$$

Note that since the power has been normalized to eliminate the inclusion of unknown drag coefficients, P is dimensionless and E has units of time. We then wish to find

$$\min_{t_0, t_f, \mathbf{x}(t)} E \quad (17)$$

subject to the constraints

$$\begin{aligned} \mathbf{x}(t_0) &= \mathbf{x}_0, \\ \mathbf{x}(t_f) &= \mathbf{x}_f, \\ ||\dot{\mathbf{x}}|| &\leq v_{\max} \\ t_{\min} \leq t_0 < t_f &\leq t_{\max}. \end{aligned}$$

This optimization problem may be solved in many ways. We have chosen to simply use existing software tools since the optimization method is not a new contribution of this paper. In the following sections, this optimization problem is input and solved in MATLAB via the use of the OPTRAGEN 2.0 [10] and SNOPT [11] toolboxes. OPTRAGEN parameterizes the trajectory using splines and translates the minimization problem to a nonlinear programming problem which is solved by SNOPT. Although this method is somewhat sensitive to the initial guess and the spline parameters used, it gives sufficiently accurate solutions for our purposes.

Note that solving this optimization problem merely gives a single optimal trajectory. This is a fuel-optimal trajectory for a single vehicle. Since we will be guiding an entire swarm of along this optimal trajectory, at most one of the vehicles in the swarm may follow the optimal trajectory. At best, the other vehicles will travel along nearly optimal trajectories.

As an estimate of the expected efficiency, we consider a trajectory $\mathbf{x}(t)$ that has been displaced from the optimal trajectory $\mathbf{x}^*(t)$ by some amount $\boldsymbol{\delta}\mathbf{x}$, but still travels at the speed required by the optimal trajectory (i.e. $\dot{\mathbf{x}} = \dot{\mathbf{x}}^*$). Due to the velocity gradients in the background flow, such a vehicle will experience a different background flow velocity than that which occurs along the optimal trajectory, and will therefore require a larger amount of energy to complete the trajectory.

A Taylor series expansion gives the background flow velocity at this displaced trajectory location to be

$$\mathbf{U}(\mathbf{x}(t), t) = \mathbf{U}(\mathbf{x}^*(t), t) + \mathbf{J}(\boldsymbol{\xi}, t)\boldsymbol{\delta}\mathbf{x} \tag{18}$$

where $\mathbf{J}$ is the Jacobian of the background velocity field and $\boldsymbol{\xi}$ is a point between $\mathbf{x}$ and $\mathbf{x}^*$. The power usage is then given by

$$P(t) = \frac{||\dot{\mathbf{x}} - (\mathbf{U}(\mathbf{x}^*(t), t) + \mathbf{J}(\boldsymbol{\xi}, t)\boldsymbol{\delta}\mathbf{x})||_2^3}{v_{\text{max}}^3}. \tag{19}$$

Let

$$\pi(t) = \frac{||\dot{\mathbf{x}}^* - \mathbf{U}(\mathbf{x}^*, t)||_2}{v_{\text{max}}} = \frac{||\dot{\mathbf{x}} - \mathbf{U}(\mathbf{x}^*, t)||_2}{v_{\text{max}}} \tag{20}$$

be the power usage of the optimal trajectory. Then

$$\begin{aligned}
P(t) \leq & \left(\frac{||\dot{\mathbf{x}} - \mathbf{U}(\mathbf{x}^*, t)||_2}{v_{\text{max}}} + \frac{||\mathbf{J}(\boldsymbol{\xi}, t)||_2 ||\boldsymbol{\delta}\mathbf{x})||_2}{v_{\text{max}}}\right)^3 \qquad (21)\\
\leq & \left(\pi(t) + \frac{||\mathbf{J}||_2 \; ||\boldsymbol{\delta}\mathbf{x})||_2}{v_{\text{max}}}\right)^3 \\
\leq & \pi^3(t) + 3\pi^2(t)\frac{||\mathbf{J}||_2 \; ||\boldsymbol{\delta}\mathbf{x}||_2}{v_{\text{max}}} \\
& + 3\pi\left(\frac{||\mathbf{J}||_2 \; ||\boldsymbol{\delta}\mathbf{x}||_2}{v_{\text{max}}}\right)^2 \\
& + \left(\frac{||\mathbf{J}||_2 \; ||\boldsymbol{\delta}\mathbf{x}||_2}{v_{\text{max}}}\right)^3.
\end{aligned}$$

Given this bound on the power usage, the total energy used by a vehicle on the trajectory $\mathbf{x}(t)$ is bounded by

$$\begin{aligned}
E \leq & E^* \qquad (22)\\
& + 3\frac{\max_t (||\mathbf{J}||_2) \; ||\boldsymbol{\delta}\mathbf{x}||_2}{v_{\text{max}}} \int_{t_0}^{t_f} \pi^2(t)dt \\
& + 3\left(\frac{\max_t (||\mathbf{J}||_2) \; ||\boldsymbol{\delta}\mathbf{x}||_2}{v_{\text{max}}}\right)^2 \int_{t_0}^{t_f} \pi(t)dt \\
& + \left(\frac{\max_t (||\mathbf{J}||_2) \; ||\boldsymbol{\delta}\mathbf{x}||_2}{v_{\text{max}}}\right)^3 (t_f - t_0)
\end{aligned}$$

where E^* is the total energy use for the optimal trajectory. Note that the integral terms in equation (22) are determined solely by the optimal trajectory and $||\mathbf{J}||_2$ is dependent on the properties of the background flow field. Of particular note is the fact that the energy bound is equal to the optimal trajectory energy usage plus three other terms involving $||\mathbf{J}||_2 \; ||\boldsymbol{\delta}\mathbf{x}||_2$. Since $||\mathbf{J}||_2$ represents the gradient of the background velocity field and $||\boldsymbol{\delta}\mathbf{x}||_2$ is the swarm size, *the trajectories are nearly optimal for velocity fields with spatial gradients that are small on the scale of the swarm size*. Put another way, the trajectories are guaranteed to be nearly optimal if $||\mathbf{J}||_2 \; ||\boldsymbol{\delta}\mathbf{x}||_2 \ll 1$

Additionally, we may achieve a better estimate of the typical energy cost by using $||\mathbf{J}||_2$ along the optimal trajectory and estimating

$$C := \frac{1}{v_{\text{max}}} R \underset{||x||_2=1}{\text{mean}} (||\mathbf{J} \; \mathbf{x}||_2) \approx \frac{||\mathbf{J} \; \boldsymbol{\delta}\mathbf{x}||_2}{v_{\text{max}}}. \tag{23}$$

The mean, $\text{mean}(||\mathbf{J} \; \mathbf{x}||_2)$, is numerically approximated along the optimal trajectory. The estimated energy use is then given by

$$\begin{aligned}
E \approx & E^* \qquad (24)\\
& + 3\int_{t_0}^{t_f} C(t)\pi^2(t)dt \\
& + 3\int_{t_0}^{t_f} C^2(t)\pi(t)dt \\
& + \int_{t_0}^{t_f} C^3(t)dt \qquad (25)
\end{aligned}$$

where C is defined by equation (23). We still expect this to be an overestimate of the fuel cost since this is based on a swarm that moves as a rigid body. In fact, the vehicle swarms are allowed to rotate and deform, further decreasing the fuel cost. Additionally, due to the finite swarm size, the vehicles in a swarm do not travel precisely between the initial and final points on the optimal trajectory. In fact, they travel from some neighborhood of the initial location to a neighborhood of the final location.

IV. Numerical simulations

To validate the control scheme presented above, we examine a simple test case via numerical simulation. This test case is chosen because it bears some similarities to the time dependent gyres that commonly appear in ocean flows. A snapshot of the velocity field is shown in figure 1. The flow consists of two counter-rotating gyres with a periodic east/west perturbation.

The velocity field for this flow is defined by the stream function

$$\psi(x, y, t) = A\sin(\pi f(x, t))\sin(\pi y) \tag{26}$$

where

$$\begin{aligned}
f(x, t) &= a(t)x^2 + b(t)x, \\
a(t) &= \epsilon \sin(\omega t), \qquad (27)\\
b(t) &= 1 - 2\epsilon \sin(\omega t).
\end{aligned}$$

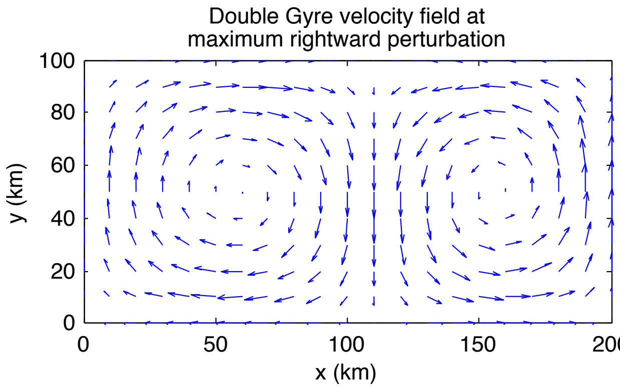

Fig. 1. The double gyre velocity field at time $t = T/4$, maximum eastward (rightward) perturbation.

The velocity field is then given by

$$u = -\frac{\partial \psi}{\partial y}, \quad (28)$$
$$v = \frac{\partial \psi}{\partial x}.$$

This velocity field is defined on the domain $[0, 2] \times [0, 1]$. To provide a more realistic scenario, the domain is rescaled to be 200 km by 100 km by simply evaluating $(u, v) = (u(x/L, y/L, t), v(x/L, y/L, t))$ where $L = 100{,}000$ m. For reference, the Red Sea is approximately 200 km wide. The flow parameters are chosen so that the maximum flow speed is 1 m/s ($A = 1/\pi$), the perturbation of the flow is about 10 km ($\epsilon = 0.1$) and the period of the time dependent oscillation is about 87 hours ($\omega = 2 \times 10^{-5}$).

Each simulation presented here is based on a vehicle or vehicle swarm beginning $x = 10$ km, $y = 10$ km and traversing the domain to reach the point $x = 150$ km, $y = 50$ km. The vehicles are given a maximum speed of 0.3 m/s. The optimal trajectory is found using OPTRAGEN and SNOPT as discussed in section III. The vehicles are given smoothing kernel values of $h = 500$ m which results in typical vehicle spacings of around 400 m. The minimum distance between any two vehicles in any of the swarms tested here was 288 m. Figure 2 shows an overview of one set of nearly optimal trajectories. This figure plots the traectories of 100 vehicles in gray, along with their positions every 12 hours (black dots), the optimal trajectory (red curve), and the goal location (red $\times$). A zoomed view of the final vehicle positions is shown so that the structure of the swarm can be seen. The vehicles closely follow the optimal trajectory with the swarm rotating and deforming slightly under the influence of the background flow. Swarms of other sizes have similar behavior.

V. Results

The main results are summarized in figures 3 and 4. Clearly, the fuel usage bound and estimate discussed in section III are overly pessimistic, with the bound quickly rising to more than an order of magnitude larger than the actual fuel usage. It is clear that the ability of the swarm to rotate and deform allows for significant fuel savings when compared to the rigid swarm approximation used to find the bound on the energy cost. Additionally, it is interesting to note that some of the vehicles achieve a fuel usage that is *below* the optimal trajectory fuel usage. This is because the vehicles do not begin and end precisely on the chosen initial and final points due to the finite size of the swarm. This results in some trajectories in the swarm that may actually require slightly less fuel than the optimal trajectory.

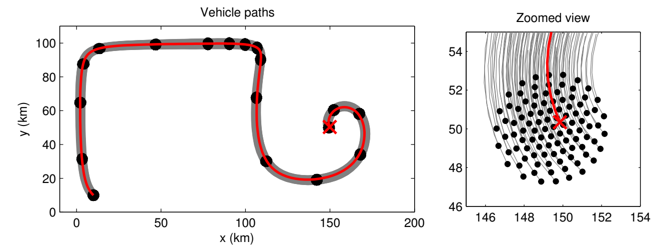

Fig. 2. An example of the nearly optimal vehicle trajectories in the double gyre flow. This figure plots the trajectories for the swarm of 100 vehicles. Vehicle trajectories are plotted as gray curves, vehicle positions are shown as black dots every 12 hours, the optimal trajectory is shown as a red curve, and the final goal location is a red $\times$. The trajectories begin at the bottom left and end at $(150, 50)$. The zoomed figure at right shows the swarm structure at the final location.

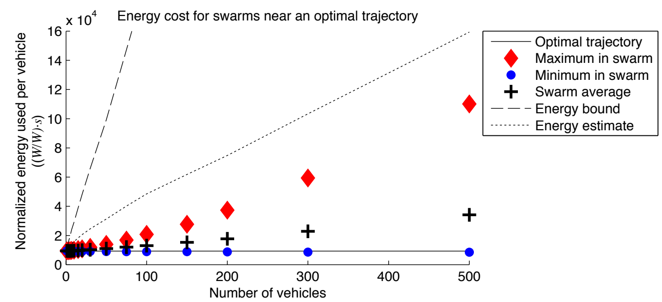

Fig. 3. The fuel cost, energy bound, and a priori energy estimate for the near optimal trajectories. The bound is a significant overestimate of the actual fuel cost while the estimated fuel cost is much closer to the true fuel requirements for vehicles in the swarm.

Despite the pessimistic bound and estimate shown in figure 3, we have still gained much insight into the expected scaling of the fuel costs. Specifically, we expect the fuel costs to behave according to the function

$$E(N) = E^* + c_1 N^{1/2} + c_2 N + c_3 N^{3/2}. \quad (29)$$

This is because the swarm radius scales as $\sqrt{N}$ as discussed in section III so substituting $R \propto \sqrt{N}$ in equations 23 and 22 and grouping all other terms into constant parameters results in equation 29. For a given vehicle spacing and scenario, we can use the data from the simulations to determine the coefficients in equation (29). Here, we use the values of the maximum or average fuel costs for swarms of $N \in \{10, 20, 50, 100\}$ vehicles to determine the coefficients of equation (29) based on the least squares best fit. The results are shown in figure 4. In each case, the the fit very accurately describes the data, even for swarms of up to 500 vehicles. The percent error in the value predicted by this fit is shown

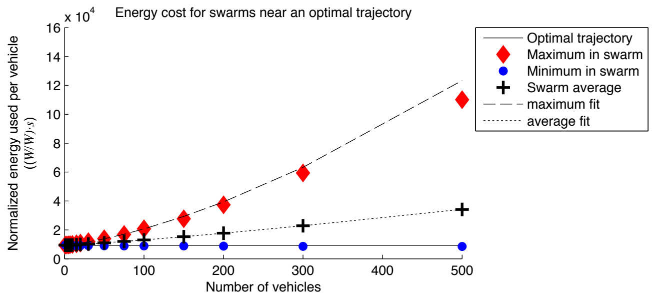

Fig. 4. The maximum, average, and minimum fuel cost for vehicles in swarms of various sizes. The curves plotted result from fitting the equation (29) to the maximum or average fuel costs for swarms of 10, 20, 50, and 100 vehicles.

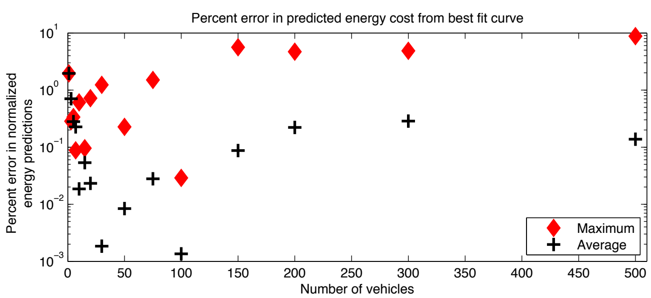

Fig. 5. The percent error in the energy cost predicted by equation (29). The coefficients were determined by a least squares best fit to the data found for swarms of 10, 20, 50, and 100 vehicles and the data and curves are shown if figure 4. The error in the predicted maximum energy cost is less than 10% while the error in the predicted average energy cost is close to 0.1%. Note: this is the error between the predicted and actual average fuel costs. Since the prediction was determined via a least squares fit based on $N \in \{10, 20, 50, 100\}$ vehicles, we expect smaller errors in this range and larger errors in the extrapolation range $N > 100$.

in figure 5. The error in the predicted maximum energy use is less than 10% for the cases tested here. The average fuel usage is more accurately predicted due to the averaging effect on random variations among vehicles, giving an error that is around 0.1% or less for most swarm sizes.

VI. Conclusions

We have developed and presented a method for near fuel-optimal trajectory planning for swarms of vehicles under the influence of a large background flow in a open domain. In flows where the velocity gradients are small on the scale of the swarm size it is possible to guide the entire swarm along a pre-computed optimal trajectory. We choose to use smoothed particle hydrodynamics (SPH) for the control algorithm. However, it is expected that artificial potential control schemes will provide similar results. We have demonstrated the capabilities of this method for simulated swarms of unmanned underwater vehicles ranging in number from one to 500 vehicles and moving through an ocean-like velocity field.

We provide an a priori bound on the fuel use for vehicles in a swarm that moves as a rigid body along the optimal trajectory. In reality, the deformability of the fluid-based SPH control scheme produces significantly more efficient trajectories than this rigid swarm approximation. The energy cost of the near optimal trajectories takes the form

$$E(N) = E^* + c_1 N^{1/2} + c_2 N + c_3 N^{3/2}$$

where E^* is the energy cost of the optimal trajectory and the constants depend on the specifics of the optimal trajectory and the gradients in the background velocity field. The coefficients in this equation can be determined via a least squares fit to a few swarm sizes. Using data for swarms of 10, 20, 50, and 100 vehicles, the coefficients are determined and provide a prediction of the maximum fuel cost that is accurate to 10% and the average fuel cost that is accurate to about 0.1%.

This method demonstrates very promising results for large swarm guidance in open domains with large velocity fields. Additionally, the SPH control scheme provides a control method that is simple to implement and allows for efficient swarm motion. The SPH scheme enables swarm guidance through the use of virtual reduced density particles and provides good collision avoidance capabilities for all test cases with a typical minimum vehicle spacing of around 400 m and a minimum observed spacing of 288 m.

References

[1] D. L. Rudnick, R. E. Davis, C. C. Eriksen, D. M. Fratantoni, and M. J. Perry, "Underwater gliders for ocean research," *Marine Technology Society Journal*, vol. 38, no. 2, pp. 73–84, 2004.

[2] J. Barraquand, B. Langlois, and J.-C. Latombe, "Numerical potential field techniques for robot path planning," *Systems, Man and Cybernetics, IEEE Transactions on*, vol. 22, no. 2, pp. 224–241, 1992.

[3] E. Gilbert and D. Johnson, "Distance functions and their application to robot path planning in the presence of obstacles," *Robotics and Automation, IEEE Journal of*, vol. 1, no. 1, pp. 21–30, 1985.

[4] P. Fiorini and Z. Shiller, "Time optimal trajectory planning in dynamic environments," in *Robotics and Automation, 1996. Proceedings., 1996 IEEE International Conference on*, vol. 2, 1996, pp. 1553–1558 vol.2.

[5] T. Inanc, J. Marsden, and S. Shadden, "Optimal trajectory generation in ocean flows," *Preprint*, 2004.

[6] D. Lipinski and K. Mohseni, "Cooperative control of a team of unmanned vehicles using smoothed particle hydrodynamics," AIAA Guidance, Navigation, and Control Conference, Toronto, Ontario, Canada, AIAA paper 2010-8316, 2-5 August 2010.

[7] B. Rhoads, I. Mezic, and A. Poje, "Minimum time feedback control of autonomous underwater vehicles," in *Decision and Control (CDC), 2010 49th IEEE Conference on*, 2010, pp. 5828–5834.

[8] J. Monaghan, "Smoothed Particle Hydrodynamics," *Annual Review of Astronomy and Astrophysics*, vol. 30, pp. 543–574, 1992.

[9] G.-R. Liu and M. Liu, *Smoothed particle hydrodynamics: a meshfree particle method*. World Scientific Publishing Company Incorporated, 2003.

[10] R. Bhattacharya, "OPTRAGEN: A MATLAB toolbox for optimal trajectory generation," in *45th IEEE Conference on Decision and Control*, San Diego, CA, USA, December 2006, pp. 6832–6836.

[11] P. Gill, W. Murray, and M. Saunders, "Snopt: An sqp algorithm for large-scale constrained optimization," *SIAM Review*, vol. 47, no. 1, pp. 99–131, 2005.